UCRL-10235

University of California

Ernest O. Lawrence Radiation Laboratory

TWO-WEEK LOAN COPY

This is a Library Circulating Copy which may be borrowed for two weeks. For a personal retention copy, call Tech. Info. Division, Ext. 5545

Berkeley, California

DISCLAIMER

This document was prepared as an account of work sponsored by the United States Government. While this document is believed to contain correct information, neither the United States Government nor any agency thereof, nor the Regents of the University of California, nor any of their employees, makes any warranty, express or implied, or assumes any legal responsibility for the accuracy, completeness, or usefulness of any information, apparatus, product, or process disclosed, or represents that its use would not infringe privately owned rights. Reference herein to any specific commercial product, process, or service by its trade name, trademark, manufacturer, or otherwise, does not necessarily constitute or imply its endorsement, recommendation, or favoring by the United States Government or any agency thereof, or the Regents of the University of California. The views and opinions of authors expressed herein do not necessarily state or reflect those of the United States Government or any agency thereof or the Regents of the University of California.

CERN- Int. Conf. on High Energy Physics.

UCRL-10235

UNIVERSITY OF CALIFORNIA
Lawrence Radiation Laboratory
Berkeley, California

Contract No. W-7405-eng-48

$\Lambda\pi^+\pi^-$ FINAL STATE IN K^--p INTERACTIONS AT K^- MOMENTA OF 1.22 AND 1.51 GeV/c

Janice Button-Shafer, Darrell Huwe, and Joseph J. Murray

June 6, 1962

$\Lambda\pi^+\pi^-$ FINAL STATE IN K^--p INTERACTIONS AT K^- MOMENTA OF 1.22 AND 1.51 GeV/c*

Janice Button-Shafer, Darrell Huwe, and Joseph J. Murray

Lawrence Radiation Laboratory
University of California
Berkeley, California

June 6, 1962

(To be presented by Harold R. Ticho)

I. INTRODUCTION

In the hydrogen bubble chamber one finds a class of K^--p events in which two charged prongs emerge from the K, p vertex, while a vee nearby appears to be the decay of a neutral particle also produced in the k, p event. One of the major reactions contributing to this class of events,

$$K^- + p \rightarrow \Lambda + \pi^+ + \pi^- \ (\Lambda 2\pi),$$

is the subject of this report. Data will be reported for K^- momenta of 1.22 and 1.51 GeV/c (μ = 1895 and 2025 MeV, respectively).

The $\Lambda 2\pi$ reactions were culled from the two prong-vee events by a two-step kinematical analysis. First by analysis of the decay vertex alone, it was possible to classify most of the vee's as Λ or K decays with 10 to 15% ambiguous and another 10 to 15% fitting neither Λ or K decay. After fulfilling the additional requirement that some Λ or K production hypothesis fit unambiguously, only about 1% of the events remained completely ambiguous. Next, in those events where the vee was identified as a Λ decay, the analytical results at the reaction vertex obtained by testing the three hypotheses $K^- + p \rightarrow \Lambda + \pi^+ + \pi^-$, $\Sigma^0 (\rightarrow \Lambda + \gamma) + \pi^+ + \pi^-$, and $\Lambda + \pi^+ + \pi^- + \pi^0$ permitted almost unambiguous classification on the basis of χ^2 alone in three categories:

*Work done under the auspices of the U.S. Atomic Energy Commission.

(Λ or Σ^0) + $\pi^+ + \pi^-$, $\Lambda + \pi^+ + \pi^- + \pi^0$, and failures (events that fit poorly for all three hypotheses). About 1% of the Λ events were ambiguous with respect to the first two categories. Individual examination of about one-fourth of the decay and production failures combined, which constitute 15 to 20% of the Λ events, shows that the reasons for their occurrence are many and varied, and that only a few percent of them are likely to turn out finally to be $\Lambda 2\pi$ reactions, but will for the most part go into other categories. In turn, we are led to believe that our final $\Lambda(\Sigma)2\pi$ samples were essentially complete and not biased significantly by failures.

Finally, Λ and $\Sigma 2\pi$ reactions were distinguished on the basis of the ratio of χ^2 for the two hypotheses. A histogram of

$$\mathcal{L} = \log_{10}\left[\frac{\chi^2(\Lambda 2\pi)}{2\chi^2(\Sigma 2\pi)}\right],$$

a parameter that a priori has no special significance, is shown in Fig. 1 for the $\Lambda(\Sigma)2\pi$ sample obtained at 1.22 GeV/c. One can see that the distribution of this parameter contains two nearly resolved peaks at -0.8 and +1.4 which can reasonably be associated respectively with true Λ and $\Sigma 2\pi$ reactions. Furthermore detailed examination of the χ^2 distributions themselves as a function of $\mathcal{L}$ indicates that our final $\Lambda 2\pi$ sample, which was defined to consist of $\Lambda(\Sigma)$ events with $\mathcal{L} < 0$, will include about 93% of the true $\Lambda 2\pi$ events and about 5% of the true $\Sigma 2\pi$ events. Essentially the same result was obtained at 1.51 GeV/c.

We have analyzed about 3200 two-prong vee events at 1.22 GeV/c and 1400 events at 1.51 GeV/c, all obtained in recent runs with the Berkeley 72-inch hydrogen bubble chamber. Summaries of the results of the foregoing analysis, together with cross sections obtained by comparison with the relative number of τ decays observed, are given in Table I.

II. COMPOSITION OF THE $\Lambda\pi^+\pi^-$ REACTIONS AND $\Lambda\pi$ MASS DISTRIBUTIONS

Here as at lower K^- momenta, the $\Lambda\pi^+\pi^-$ final state of the K^-–p reaction is dominated by production of Y_1^*, the T = 1 $\Lambda\pi$ resonance first observed by Alston et al.[1] In Figs. 2 and 3 are shown histograms of the effective[2] invariant mass of the $\Lambda\pi^+$ and $\Lambda\pi^-$ pairs observed with P_K = 1.2 GeV/c. The solid curves are three-body relativistic phase space, and the same phase space modified by a resonance function of the form $[(M_{\Lambda\pi}-M_{Y^*})^2+(\Gamma/2)^2]^{-1}$. The fits shown were obtained assuming no background, with a ratio Y^{*+}/Y^{*-} equal to 0.85 and with M_{Y^*} = 1385 MeV and $\Gamma/2$ = 25 MeV, the latter two values in agreement with previous measurements. Our mass resolution, $\Gamma_{res} \approx 5$ MeV, contributes negligibly to the observed width.

Similar results, shown in Figs. 7 and 8, were obtained at 1.51 GeV/c with much less data, but with significant differences in two respects. For one thing, the ratio Y^{*+}/Y^{*-} increased to about 1.2 ± 0.15. Perhaps more significant is the fact that the mass distributions are not so well accounted for by the simple phase space-resonance model as at 1.22 GeV/c, with the implication that a background comes in at 1.51 GeV/c that is as large as 10 to 20% of the total number of $\Lambda\pi^+\pi^-$ events.

PRODUCTION ANGULAR DISTRIBUTION FOR Y^* EVENTS

In Fig. 4 are shown the production angular distributions for $Y^{*\pm}$ events at both 1.22 and 1.51 GeV/c, where Y^* events are defined to be those in which the effective mass of a $\Lambda\pi$ pair lies between the limits 1340 and 1430 GeV. Least-squares fits up to the fourth power in $\hat{Y}^* \cdot \hat{K}$ were obtained at 1.22 GeV/c whose coefficients are listed in Table II, presented for comparison along with corresponding results obtained by Ely et al. at 1.1 GeV/c.[3] The presence of significant negative coefficients for the fourth-power term can be associated

directly with the falloff in the angular distribution as $\hat{Y}^* \cdot \hat{K} \rightarrow -1.0$ and this, as pointed out by Ely et al., is characteristic of $D_{5/2}$ wave production of a $J = 3/2$ resonance. We do not believe the falloff is the result of bias.

Too few data are as yet available at 1.51 GeV/c to permit detailed conclusions but the general shape of the production angular distributions there appear to be essentially the same as at 1.22 GeV/c.

Y^* DECAY ANGULAR DISTRIBUTIONS WITH RESPECT TO THE PRODUCTION NORMAL

If its spin were 1/2, and in the absence of interfering background, the Y_1^* must necessarily decay isotropically with respect to the production normal $\hat{n} = (\hat{K} \times \hat{Y}^*)/|\hat{K} \times \hat{Y}^2|$. Evidence has been presented favoring Y_1^* spin $\geqslant 3/2$ by Ely et al.,[3] however, who find that at $p_K = 1.1$ GeV/c the Y_1^* decay with respect to the production normal is not isotropic, but fits the form $1 + a \cos^2 \theta$ with $a = 1.5 \pm 0.4$. Corresponding Y_1^* decay angular distributions observed at $p_K = 1.22$ and 1.51 GeV/c are shown in Fig. 5, with values of a obtained from best fits to the form $1 + a \cos^2 \theta$ listed in Table III.

Our results could not fail to be consistent with the conclusion of Ely, et al.,[3] but alone they would probably be considered to be inconclusive with respect to the spin of Y_1^*.

Y^* DECAY ANGULAR DISTRIBUTION WITH RESPECT TO THE Y^* DIRECTION OF MOTION

As may be seen from Fig. 6 and Table IV, Y^* decay with respect to its own direction of motion is significantly asymmetric at $P_K = 1.22$ GeV/c, indicating that here, as at lower momenta, the concept of "free" decay of the Y^* has limited validity. It would appear, however, that at 1.22 GeV/c the observed asymmetry could be accounted for as a result of interference between Y_1^{*+} and Y_1^{*-} amplitudes. On the other hand, the striking increase

in asymmetry of the corresponding decay for Y^{*-}, and the apparent change in character of the distribution for Y^{*+} at 1.51 GeV/c, probably cannot be accounted for in the same way. It is possible that these effects are another manifestation of interfering background noted previously in connection with the interpretation of the $\Lambda\pi$ mass distribution. The ρ meson production could account for an interfering background, and although data are as yet too few to conclude that such is indeed the case, an upper limit on ρ production at 1.51 GeV/c, ample to account for the observed "background" effects, is about 200 μb. On the other hand, at 1.22 GeV/c where the results are consistent with no background, an upper limit for any sharply resonant dipion production is about 100 μb.

NEGATIVE RESULTS

Analyses of Adair distributions at 1.22 GeV/c were inconclusive and the data 1.51 GeV/c are too few to be considered seriously in this respect. Unfortunately also, no significant average polarization of the Λ or correlation of Λ polarization with Y^* production angle was found at either 1.22 or 1.51 GeV/c.

ACKNOWLEDGMENT

We would like to acknowledge the very valuable assistance of Dr. Stanley Wojcicki in the analysis of data presented here.

REFERENCES AND FOOTNOTES

1. Alston et al., Phys. Rev. Letters 5, 520 (1960).
2. The "effective" in the present context means as calculated from fitted values of the Λ and π parameters. obtained from kinematical analysis testing the $\Lambda\pi^+\pi^-$ hypothesis.
3. Robert P. Ely et al., Phys. Rev. Letters 7, 461 (1961).

Table I. Composition of Two Prong-vee $\bar{K}$, p Events and the $\Lambda\pi^+\pi$ Cross Sections at 1.22 and 1.51 GeV/c.

P_K (GeV/c)	Two-prong vee events analyzed (No.)	$\Lambda 2\pi$ (No.)	$\Sigma 2\pi$ (No.)	$\Lambda 3\pi$ (No.)	Failures (No.)	$\sigma(\Lambda\pi^+\pi^-)$ (mb)
1.22	3200	1380	570	350	323	2.2 ± .2
1.51	1400	300	150	320	170	1.4± .3

Table II. Coefficients of powers of $\cos\theta = \hat{Y}^* \cdot \hat{K}$ in fitted production angular distributions for Y^{*+} and Y^{*-} at 1.22 GeV/c, compared with corresponding distributions of Ely et al.[a] at 1.15 GeV/c.

	1	$\cos\theta$	$\cos\theta^2$	$\cos\theta^3$	$\cos\theta^4$	
Y^{*+}	8.0 ± 1.2	-17.4± 3.8	65.0 ± 10.0	20.0 ± 5.8	-57.4 ± 10.6	This experiment
	7.9 ± 1.9	-19.9± 5.7	62.1± 16.1	22.6 ± 8.9	-63.0± 19.7	Ely et al.
Y^{*-}	9.4 ± 1.0	-11.6 ± 2.9	35.0 ± 7.5	4.6 ± 4.6	-30.0 ± 8.7	This experiment
	15.5 ± 2.0	-0.1 ± 6.0	15.5 ± 5.1	21.9 ± 9.7	———	Ely et al

[a] R. P. Ely et al., Phys. Rev. Letters 7, 461 (1961).

Table III. Coefficients of $\cos^2\theta = (\hat{\Lambda}\cdot\hat{n})^2$, $\hat{n} = (\hat{K}\times\hat{Y}^*)/|\hat{K}\times\hat{Y}^*|$ in the decay angular distributions of Y_1^* with respect to the production normal fitted to the form $1 + a\cos^2\theta$.

p_K GeV/c	Y^{*+}	Y^{*-}
1.22	0.48 ± 0.36	0.51 ± 0.33
1.51	0.4 ± 0.6	0.4 ± 0.8

Table IV. Values of $b = 3\ [\hat{\Lambda}\cdot\hat{Y}^*]_{av}$ for the decay angular distribution of Y^* with respect to its own direction of motion.

p_K GeV/c	Y^{*+}	Y^{*-}
1.22	-0.23 ± 0.08	-0.17 ± 0.07
1.51	—	-0.54 ± 0.2

FIGURE CAPTIONS

Fig. 1. Distribution of the parameter $\mathcal{L} = \log_{10} [\chi^2(\Lambda 2\pi)/2\chi^2(\Sigma 2\pi)]$ for 1943 reactions of the type $K^- + p \rightarrow \Lambda(\Sigma) + \pi^+ + \pi^-$, with $\chi^2(\Lambda 2\pi) < 40$, or $\chi^2(\Sigma 2\pi) < 20$, at a K^- momentum of 1.22 GeV/c (μ = 1895 MeV.) The nearly resolved peaks at $\mathcal{L} = -0.8$ and $+1.4$ are associated respectively with true $\Lambda 2\pi$ and $\Sigma 2\pi$ reactions.

Fig. 2. Effective mass distribution for the $\Lambda\pi^+$ pair in the reaction $K^- + p \rightarrow \Lambda + \pi^+ + \pi^-$ at p_K = 1.22 GeV/c. Solid curves are three-body relativistic phase space and the same phase space modified by a resonance function of the form $[(M_{\Lambda\pi} - M_{Y^*})^2 + (\Gamma/2)^2]^{-1}$, with M_{Y^*} = 1385 MeV, $\Gamma/2$ = 25 MeV, and $Y^{*+}/Y^{*-} = 0.85$.

Fig. 3. Effective mass distribution for the $\Lambda\pi^-$ pair in the reaction $K^- + p \rightarrow \Lambda + \pi^+ + \pi^-$ at P_K = 1.22 GeV/c. See Fig. 2 for explanation of the solid curves.

Fig. 4. Production angular distribution for Y^* events in the reaction $K^- + p \rightarrow \Lambda + \pi^+ + \pi^-$. Y^* events are defined as those for which the effective mass of a $\Lambda\pi$ pair lies between the limits 1340 and 1430 MeV. The solid curves at 1.22 GeV/c are fits through $\cos^4$, whose coefficients are listed in Table II.

Fig. 5. Angular distributions of Y^* decay with respect to the production normal $\hat{n} = (\hat{K} \times \hat{Y}^*)/|\hat{K} \times \hat{Y}^*|$ for "equatorially" produced events in which $|\hat{Y}^* \cdot \hat{K}| < 0.5$. Solid curves are normalized best fits to the form $1 + a(\hat{\Lambda} \cdot \hat{n})^2$, with values of $\underline{a}$ given in Table III.

Fig. 6. Angular distributions of the Λ from Y^* decays with respect to the Y^* direction of motion for all Y^* events; that is, those events for which the effective mass of a $\Lambda\pi$ pair was between 1340 and 1430 MeV. Solid curves are normalized functions of the form $1 + b(\hat{\Lambda} \cdot \hat{Y}^*)$, where the

values of $b = 3\,[\hat{\Lambda} \cdot \hat{Y}^*]_{av}$ are given in Table IV.

Fig. 7. Effective mass distribution for the $\Lambda\pi^+$ pair in the reaction $K^- + p \rightarrow \Lambda + \pi^+ + \pi^-$ at $p_K = 1.51$ GeV/c. Solid curve is relativistic phase space modified by a resonance function of the form $[(M_{\Lambda\pi} - M_{Y^*})^2 + (\Gamma/2)^2]^{-1}$ with $M_{Y^*} = 1385$ MeV, $\Gamma/2 = 25$ MeV, and $Y^{*+}/Y^{*-} = 1.2$.

Fig. 8. Effective mass distribution for the $\Lambda\pi^-$ pair in the reaction $K^- + p \rightarrow \Lambda + \pi^+ + \pi^-$ at $p_K = 1.51$ GeV/c. See Fig. 7 for explanation of the solid curve.

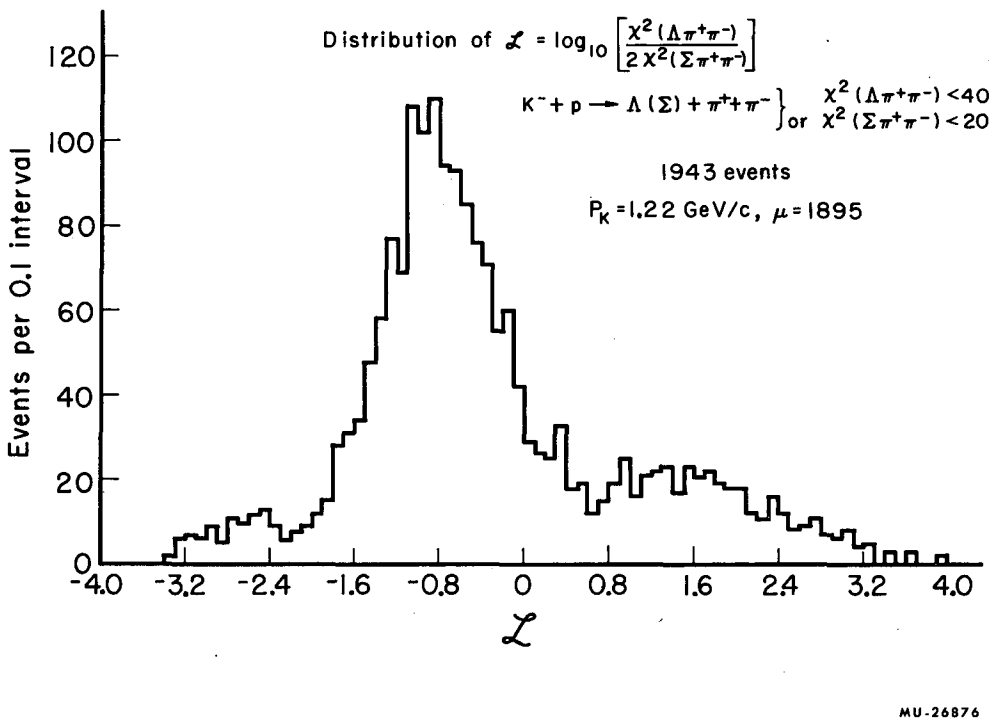
Distribution of $\mathcal{L} = \log_{10}\left[\frac{\chi^2(\Lambda\pi^+\pi^-)}{2\chi^2(\Sigma\pi^+\pi^-)}\right]$
$K^- + p \rightarrow \Lambda(\Sigma) + \pi^+ + \pi^-$ $\chi^2(\Lambda\pi^+\pi^-) < 40$ or $\chi^2(\Sigma\pi^+\pi^-) < 20$
1943 events
$P_K = 1.22$ GeV/c, $\mu = 1895$
Events per 0.1 interval
120
100
80
60
40
20
0
-4.0
-3.2
-2.4
-1.6
-0.8
0
0.8
1.6
2.4
3.2
4.0
$\mathcal{L}$
MU-26876

Fig. 1

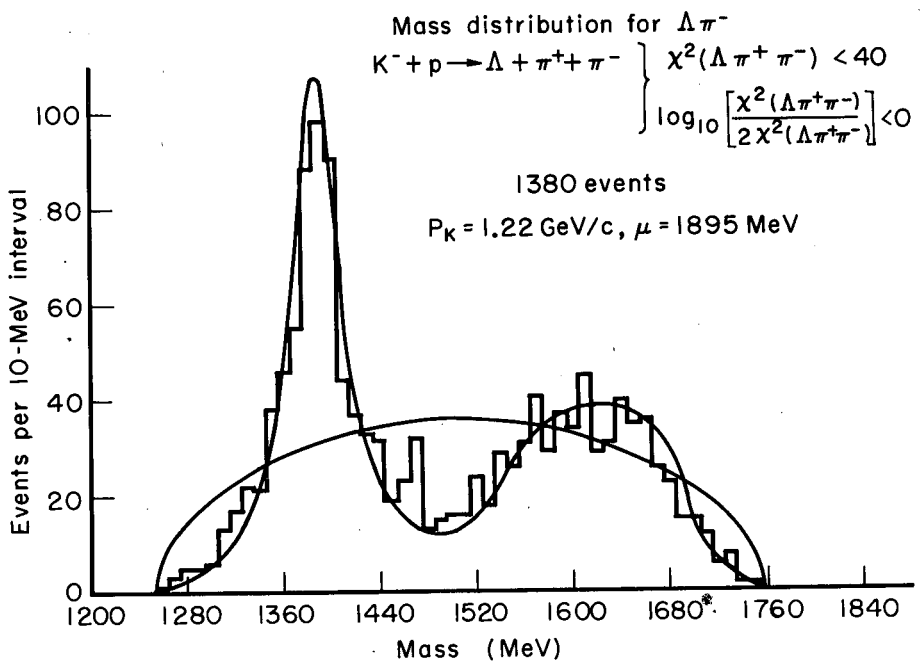

MU-26877

Fig. 2

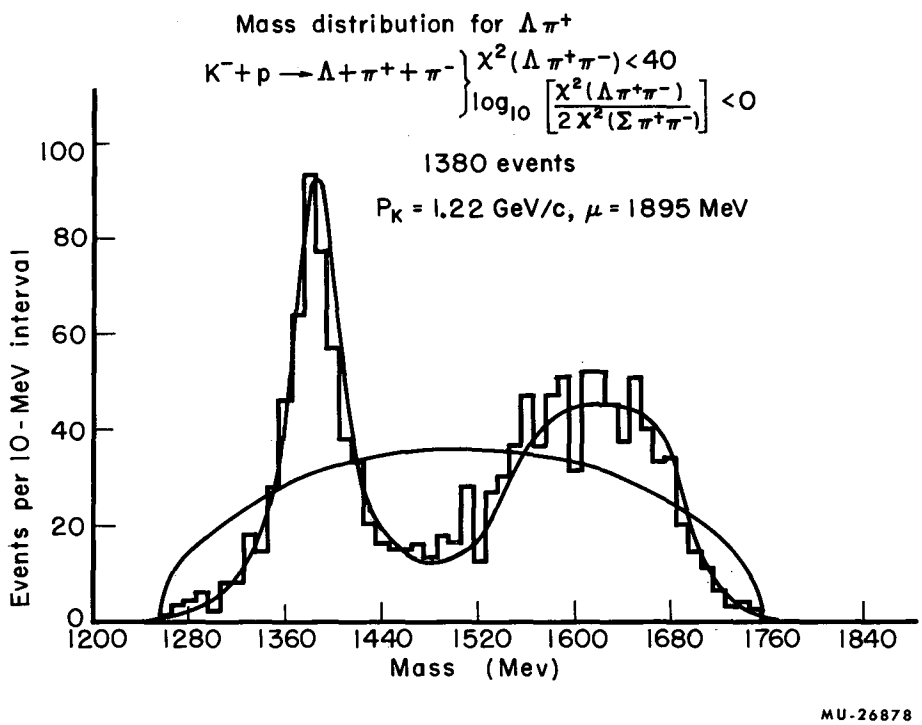
Mass distribution for $\Lambda\pi^+$
$K^- + p \rightarrow \Lambda + \pi^+ + \pi^-$ $\chi^2(\Lambda\pi^+\pi^-) < 40$
$\log_{10}\left[\frac{\chi^2(\Lambda\pi^+\pi^-)}{2\chi^2(\Sigma\pi^+\pi^-)}\right] < 0$
1380 events
P_K = 1.22 GeV/c, μ = 1895 MeV
Events per 10-MeV interval
0
20
40
60
80
100
1200
1280
1360
1440
1520
1600
1680
1760
1840
Mass (Mev)
MU-26878

Fig. 3

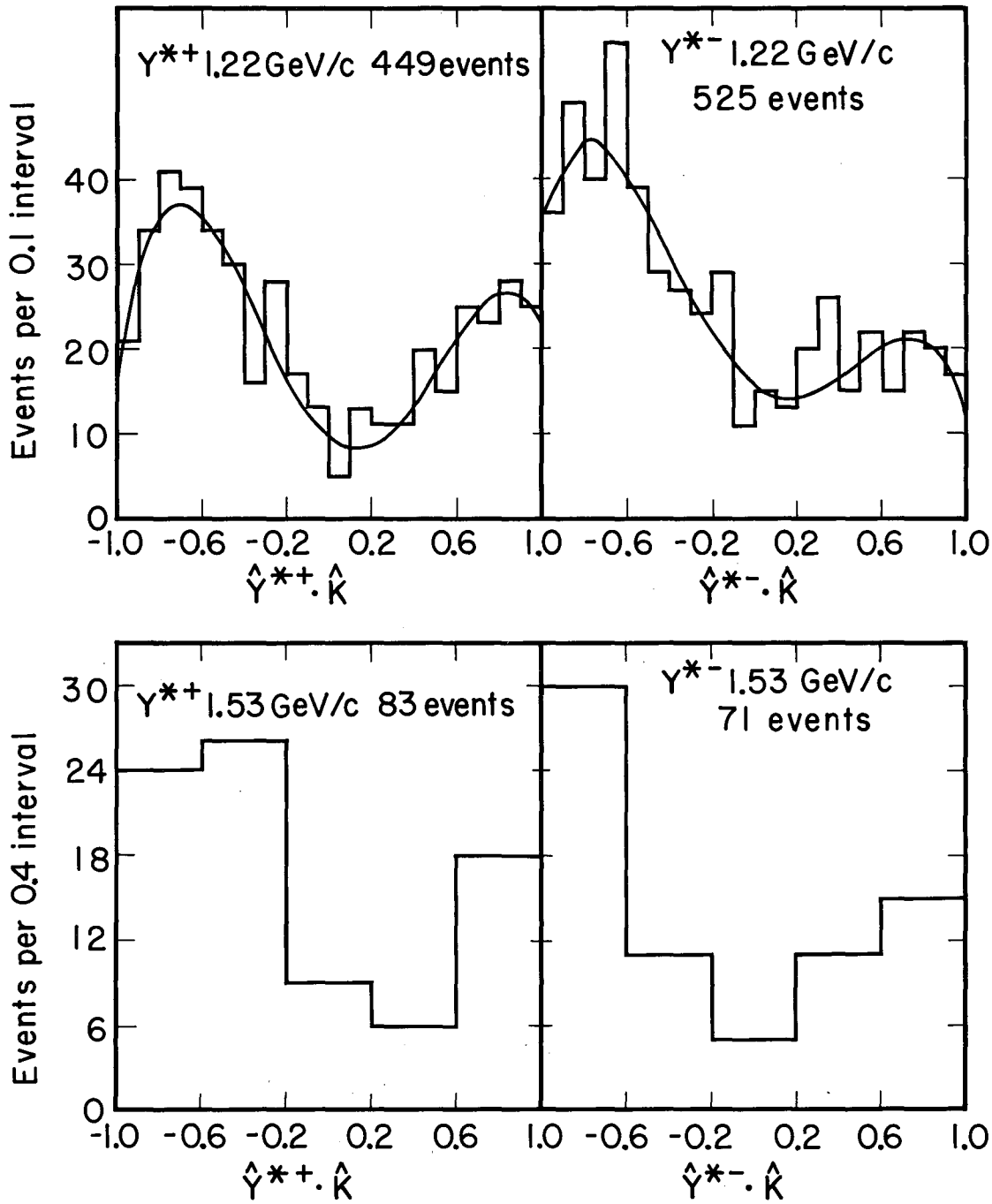

MUB-1098

Fig. 4

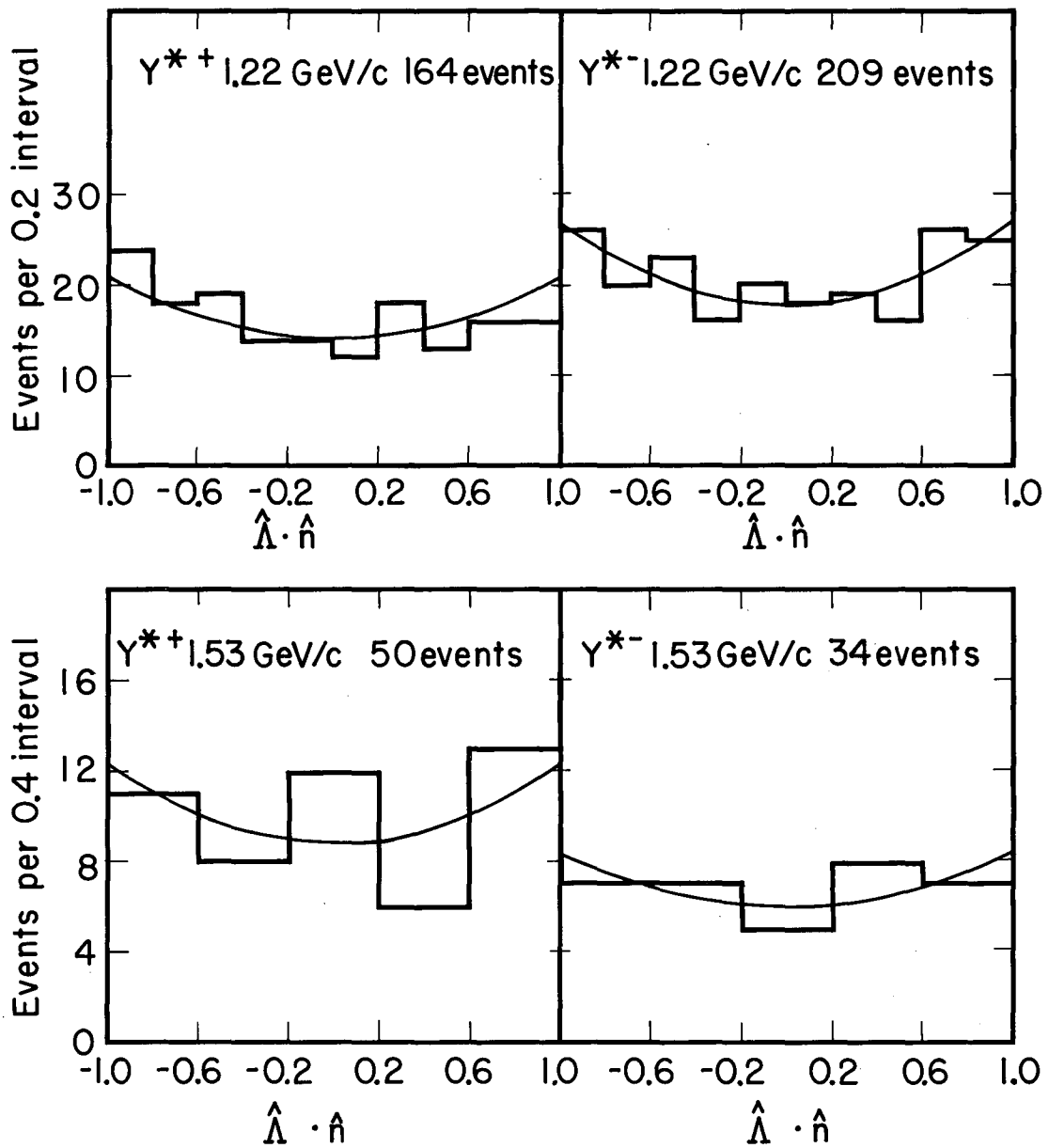

MUB-1099

Fig. 5

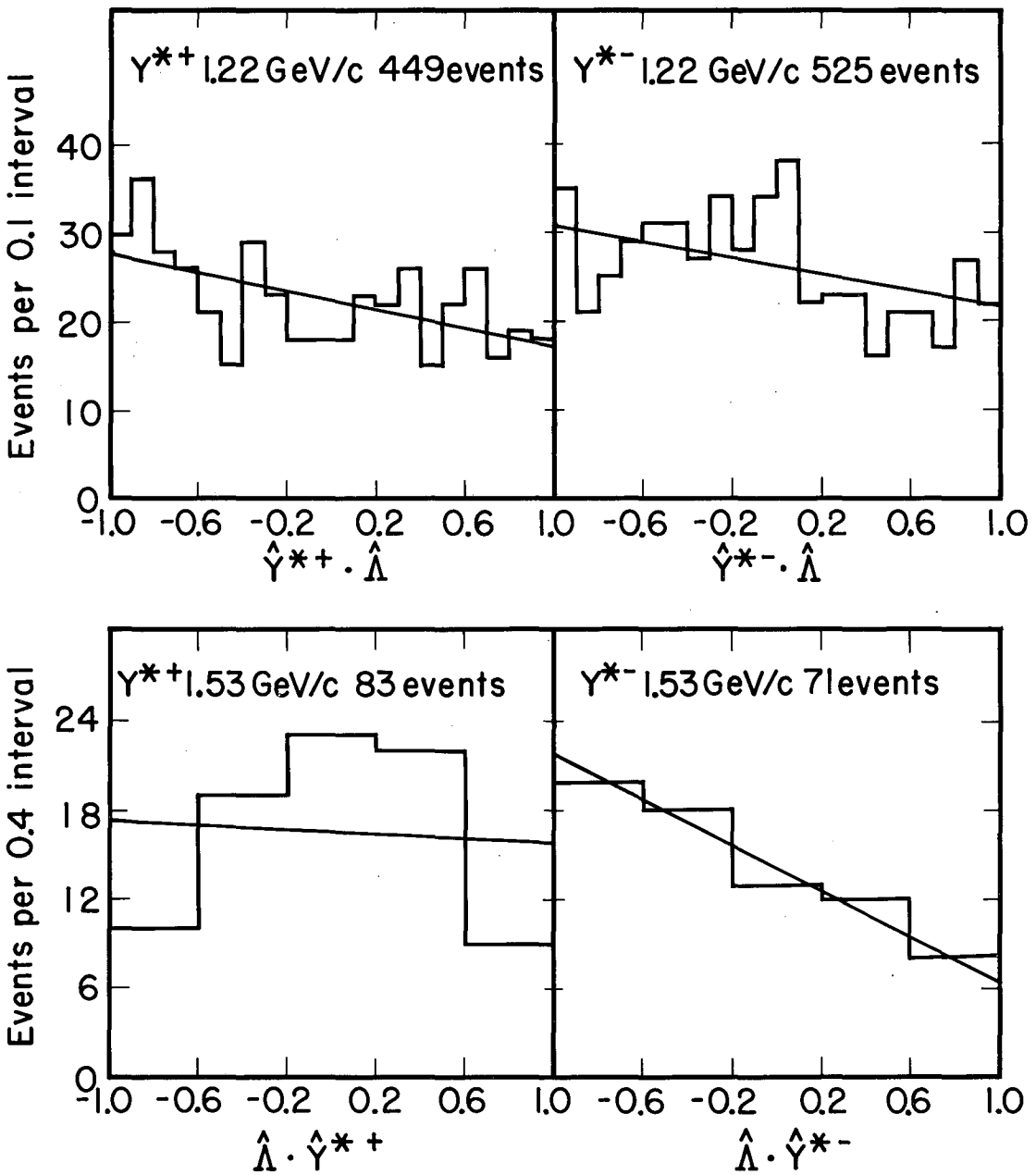
Y*+ 1.22 GeV/c 449 events
Y*- 1.22 GeV/c 525 events
Events per 0.1 interval
40
30
20
10
0
-1.0 -0.6 -0.2 0.2 0.6 1.0
Ŷ*+ · Λ̂
Ŷ*- · Λ̂
Y*+ 1.53 GeV/c 83 events
Y*- 1.53 GeV/c 71 events
Events per 0.4 interval
24
18
12
6
0
Λ̂ · Ŷ*+
Λ̂ · Ŷ*-
MUB-1097

Fig. 6

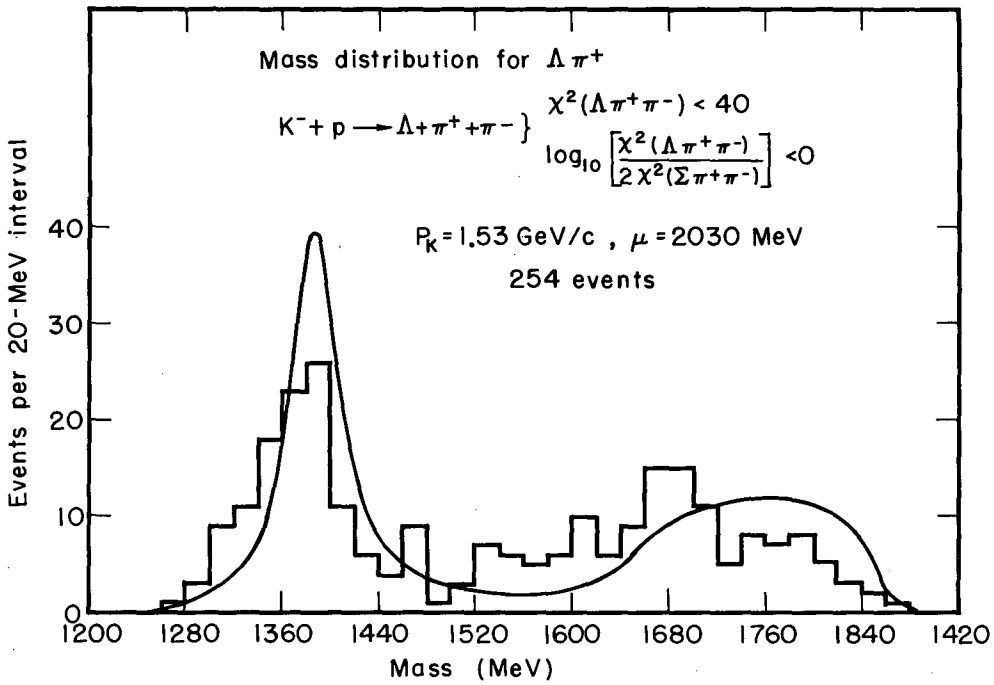

MU-27093

Fig. 7

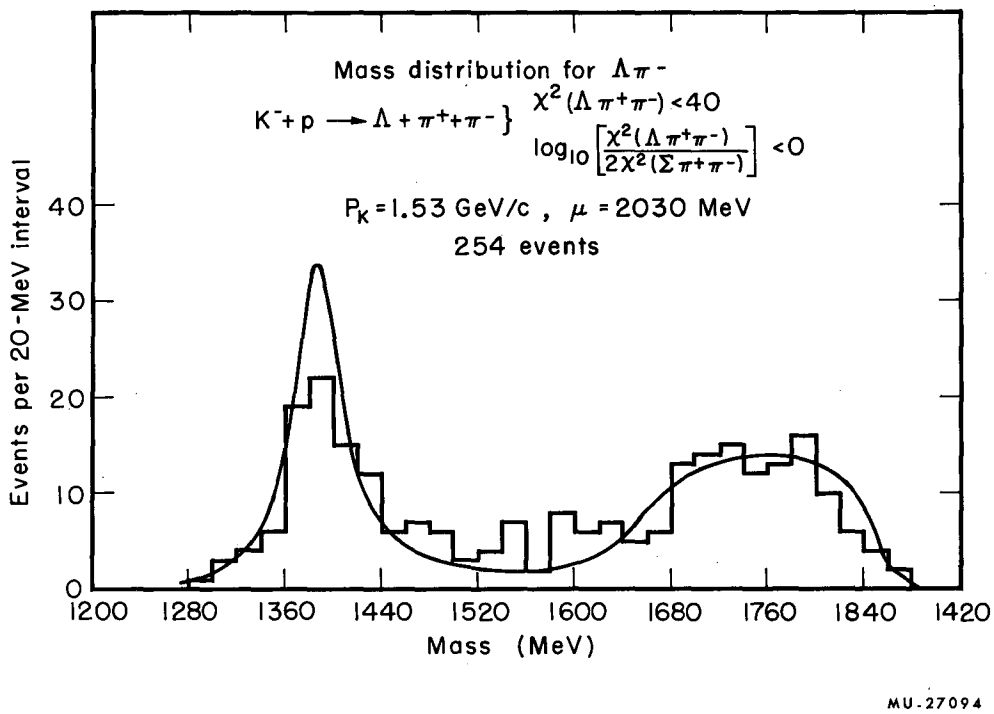
Mass distribution for $\Lambda\pi^-$
$K^- + p \rightarrow \Lambda + \pi^+ + \pi^-$ } $\chi^2(\Lambda\pi^+\pi^-) < 40$
$\log_{10}\left[\frac{\chi^2(\Lambda\pi^+\pi^-)}{2\chi^2(\Sigma\pi^+\pi^-)}\right] < 0$
$P_K = 1.53$ GeV/c , $\mu = 2030$ MeV
254 events
Events per 20-MeV interval
0
10
20
30
40
1200
1280
1360
1440
1520
1600
1680
1760
1840
1420
Mass (MeV)
MU-27094

Fig. 8

This report was prepared as an account of Government sponsored work. Neither the United States, nor the Commission, nor any person acting on behalf of the Commission:

A. Makes any warranty or representation, expressed or implied, with respect to the accuracy, completeness, or usefulness of the information contained in this report, or that the use of any information, apparatus, method, or process disclosed in this report may not infringe privately owned rights; or

B. Assumes any liabilities with respect to the use of, or for damages resulting from the use of any information, apparatus, method, or process disclosed in this report.

As used in the above, "person acting on behalf of the Commission" includes any employee or contractor of the Commission, or employee of such contractor, to the extent that such employee or contractor of the Commission, or employee of such contractor prepares, disseminates, or provides access to, any information pursuant to his employment or contract with the Commission, or his employment with such contractor.